MNRAS **000**, 000–000 (0000) Preprint 10 June 2018 Compiled using MNRAS LATEX style file v3.0

Prospects for cosmic magnification measurements using HI intensity mapping

10 June 2018

ABSTRACT

We investigate the prospects of measuring the cosmic magnification effect via cross-correlating 21cm intensity mapping foreground maps with background optical galaxies.

Key words: cosmology: large-scale structure of the universe

1 INTRODUCTION

blabla

2 FORMALISM

2.1 Cosmic Magnification: galaxies

Using galaxies as biased tracers of matter, cosmic magnification is the effect of lensing in the observed galaxy distribution. Lensing magnification makes galaxies appear brighter, which means that objects that are dimmer than the flux cut-off of a given survey can be detected, so that their observed number density increases. However, the apparent area is also increased, therefore the observed number density of galaxies decreases. Formalising the above description we can write the observed galaxy number overdensity as (Ziour & Hui 2008)

$$\delta_{\rm g}^{\rm L} = \delta_{\rm g} + (5s_{\rm g} - 2)\kappa + \mathcal{O}(\kappa^2)\,, \qquad (1)$$

with $\delta_{\rm g}$ the intrinsic galaxy overdensity and κ the lensing convergence. The quantity $s_{\rm g}$ is the number count slope, which for a survey with limiting magnitude $m_\star$ is

$$s_{\rm g} = \frac{d\log_{10}N(<m_\star)}{dm_\star}\,. \qquad (2)$$

Cross-correlating well separated foreground (f) and background (b) galaxy samples we can eliminate the intrinsic galaxy overdensity correlation term $\langle\delta_{\rm g}(\theta_{\rm f},z_{\rm f})\delta_{\rm g}(\theta_{\rm b},z_{\rm b})\rangle$ and get

$$\begin{aligned}\langle\delta_{\rm g}^{\rm L}(\theta_{\rm f},z_{\rm f})\delta_{\rm g}^{\rm L}(\theta_{\rm b},z_{\rm b})\rangle &= (5s_{\rm g}^{\rm b}-2)\langle\kappa_{\rm b}\delta_{\rm g}(\theta_{\rm f},z_{\rm f})\rangle \\ &+ (5s_{\rm g}^{\rm f}-2)(5s_{\rm g}^{\rm b}-2)\langle\kappa_{\rm f}\kappa_{\rm b}\rangle\,. \qquad (3)\end{aligned}$$

The first term on the right hand side of the above equation is the magnification-galaxy (μg) correlation, while the second term is the magnification-magnification ($\mu\mu$) correlation. In many cases the later can be neglected because it is much smaller than the μg term, but as the redshift of the foreground galaxies increases it becomes important (Ziour & Hui 2008). An 8σ detection of the cosmic magnification effect was achieved in Scranton et al. (2005) using the Sloan Digital Sky Survey and the galaxy-quasar cross-correlation.

Measurements of the μg correlation are useful to constrain the galaxy-mass power spectrum. The method is complementary to galaxy-galaxy shear measurements, being free from many systematic errors that affect shear measurements such as point spread function and galaxy intrinsic alignment.

2.2 Cosmic Magnification: intensity mapping

Instead of galaxies, we can consider HI as a biased tracer of matter. Using intensity mapping to probe the 21cm temperature (intensity) fluctuations, there is no lensing contribution at linear order because surface brightness is conserved (Hall et al. 2013). This means we can write $s_{\rm HI} = 2/5$ and - assuming an HI foreground sample and a galaxy background sample - we have

$$\delta T_{21}^{\rm L} = \delta T_{21} = \bar{T}_b\delta_{\rm HI} = \bar{T}_b b_{\rm HI}\delta\,, \qquad (4)$$

where $\bar{T}_b$ is the mean brightness temperature. Hence

$$\langle\delta_{\rm HI}^{\rm L}(\theta_{\rm f},z_{\rm f})\delta_{\rm g}^{\rm L}(\theta_b,z_b)\rangle = (5s_{\rm g}^{\rm b}-2)\langle\kappa_b\delta_{\rm HI}(\theta_{\rm f},z_{\rm f})\rangle\,. \qquad (5)$$

Note the absence of the magnification-magnification term since $s_{\rm HI}^{\rm f} = 2/5$. This means that the above relation is exact at all redshifts, provided that the foreground and background samples are well separated. This can be guaranteed via the excellent redshift information provided by the intensity mapping survey.

We can express the signal we are after using the angular power spectrum Ziour & Hui (2008)

$$C_\ell^{{\rm HI}-\mu}(z_{\rm f},z_{\rm b}) = \frac{3}{2}\frac{H_0^2}{c^2}\Omega_{\rm m,0}\times \int_0^\infty dz\frac{b_{\rm HI}(z)W(z,z_{\rm f})g(z,z_{\rm b})}{r^2(z)}(1+z)P((\ell+1/2)/r(z),z) \qquad (6)$$

where we have employed the Limber approximation, valid for $\ell \geqslant 10$ (Limber 1954; Loverde & Afshordi 2008). The function $W(z,z_{\rm f})$ is the foreground sources redshift distri-

bution, while $g(z, z_\mathrm{b})$ is the lensing kernel given by

$$g(z, z_\mathrm{b}) = r(z) \int_z^\infty dz' \frac{r(z') - r(z)}{r(z')} (5s_\mathrm{g}(z') - 2) W(z', z_\mathrm{b}) \,. \tag{7}$$

The error in the measurement of the power spectrum is

$$\Delta C_\ell^{\mathrm{HI}-\mu} = \sqrt{\frac{2((C_\ell^{\mathrm{HI}-\mu})^2 + (C_\ell^{\mathrm{gg}} + C^{\mathrm{shot}})(C_\ell^{\mathrm{HI-HI}} + N_\ell))}{(2\ell+1)\Delta\ell f_\mathrm{sky}}} \,, \tag{8}$$

where C^{shot} the galaxy shot noise power spectrum, N_ℓ the thermal noise of the intensity mapping instrument, $\Delta\ell$ the binning in multipole space, and f_sky the fraction of the sky the surveys scan.

$$C_\ell^{\mathrm{HI-HI}} = \frac{H_0}{c} \int dz E \left(\frac{b_\mathrm{HI}(z) W(z) T_\mathrm{obs} D}{r} \right)^2 P_\mathrm{cdm} \left(\frac{\ell + 1/2}{r} \right) \tag{9}$$

Where the HI bias is given by the fit from ???

$$b_\mathrm{HI}(z) = 0.67 + 0.18z + 0.05z^2 \tag{10}$$

$$C_\ell^{\mathrm{gg}} = \frac{H_0}{c} \int dz E \left(\frac{b_\mathrm{g}(z) W(z) D}{r} \right)^2 P_\mathrm{cdm} \left(\frac{\ell + 1/2}{r} \right) \tag{11}$$

We use the galaxy bias b_g from Alonso et al. (2015).

3 EXPERIMENTS AND NOISE CALCULATIONS

We use HIRAX and SKA and pair them with LSST. For HIRAX we assume a 1024 and a 512 dish setup, full correlation, a system temperature $T_\mathrm{sys} = 50$ mK, a dish diameter of $D_\mathrm{dish} = 6$ m, a compact square grid baseline with 1 m space between dishes and a sky fraction $f_\mathrm{sky} = 1/4$. Its frequency range is from 400 to 800 MHz and we use equally spaced redshift bins of width $dz = 0.1$. The autocorrelation experiment SKA is assumed to consist of the 64 MeerKAT 13.5 m dishes and 133 15 m dishes. The system temperature is assumed to be constant at $T_\mathrm{sys} = 30$ mK in the relevant redshift range (low). For the beam calculation we use $\tilde{D}_\mathrm{dish} = (64 * 13.5 + 133 * 15)/(64 + 133)$. The SKA sky fraction is assumed to be $f_\mathrm{sky} = 0.6$. We consider two frequency ranges for SKA: Band 1 from 580 to 1015 MHz and band 2 from 950 to 1420 MHz. For all experiments we assumed a total integration time of $t_\mathrm{tot} = 10000$ h and full survey overlap with LSST.

For SKA we calculate the single dish noise

$$N_\ell^\mathrm{SD} = \sigma_\mathrm{pix}^2 \Omega_\mathrm{pix} W_\ell^{-1}, \tag{12}$$

with the area per pixel $\Omega_\mathrm{pix} = 4\pi/N_\mathrm{pix}$, the number of pixels N_pix, the beam smoothing function $W_\ell = \exp\left(-\ell^2 \Theta_\mathrm{FWHM}^2/(8 \ln 2)\right)$ and the pixel noise $\sigma_\mathrm{pix} = T_\mathrm{sys} * \sqrt{N_\mathrm{pix} f_\mathrm{sky}/(t_\mathrm{tot} \delta_\nu N_\mathrm{dish})}$.

For HIRAX we calculate the interferometer noise as

$$N_\ell^\mathrm{i} = \frac{(\lambda^2 T_\mathrm{sys})^2}{2 A_\mathrm{e}^2 d\nu n(u), t_\mathrm{p}} \tag{13}$$

with the frequency bin width $d\nu$, the time per pointing $t_\mathrm{p} = t_\mathrm{tot}/N_\mathrm{p}$, the effective collecting area of one dish $A_\mathrm{e} = (D_\mathrm{dish}/2)^2 \pi$, the baseline density $n(u)$ of $u = \ell/(2\pi)$.

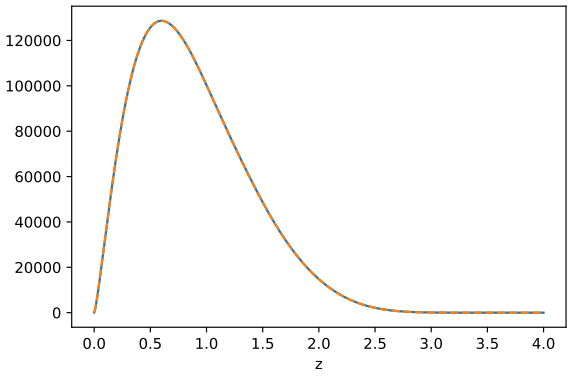

Figure 1. LSST dN/dz.

AP: We should also probably use a more realistic W (not top-hat) for LSST, although I don't think it will make a big difference.AW: We agreed it should only matter if we use small background bins

The galaxy shot noise is calculated as $C^{\mathrm{shot}} = 4\pi/N^{\mathrm{LSST}}(z)$, with N_i^{LSST} the number of detected galaxies in the considered redshift bin i. All LSST redshift bins go up to $z_\mathrm{max}^{\mathrm{LSST}} = 3.7$, and start at a small separation from the upper edge of the foreground bin, $z_i^{\mathrm{fg}} + 0.1$. The choice of a separation distance of 0.1 is conservative, ruling out any cross correlations from possible overlaps, for example from the photometric redshifts. We calculate the number count slope for LSST by fitting the s_g given in Alonso et al. (2015).

4 RESULTS

In figure 5 we show the signal to noise for all different experiment combinations. All foreground experiments are correlated with one single, non-overlapping redshift bin of LSST. Low redshift foregrounds bins perform better than high redshift bins, especially in the case for HIRAX, where the LSST shot noise becomes the dominant source of error. The 512 dish HIRAX performs surprisingly well, as even in this case the interferometer noise remains subdominant. The solid black line shows the cosmic variance limit (for both foreground and background surveys), and the grey shaded area indicates the start of nonlinear regime, which depends on redshift. We calculate the nonlinear scale according to (), $k_\mathrm{NL}(z) = k_\mathrm{NL,0}(1+z)^{2/(2+n_\mathrm{s})}$, where n_s is the spectral index of primordial scalar perturbations, and $k_\mathrm{NL,0} = 0.14$ Mpc^{-1}.

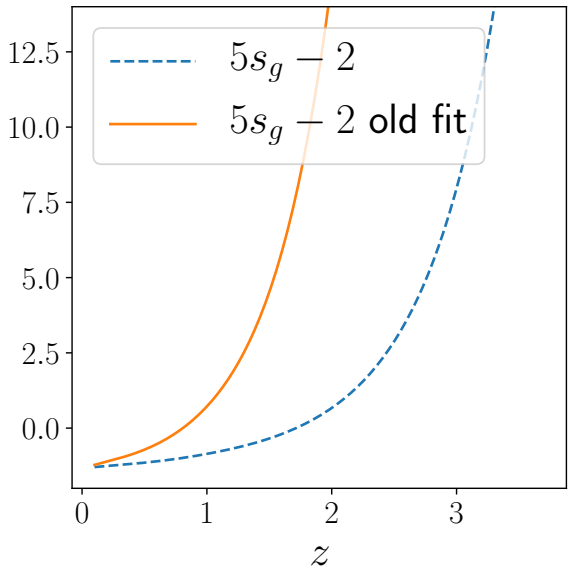

Figure 2. The s_g we used (from Ze) VS the one we use for LSST.

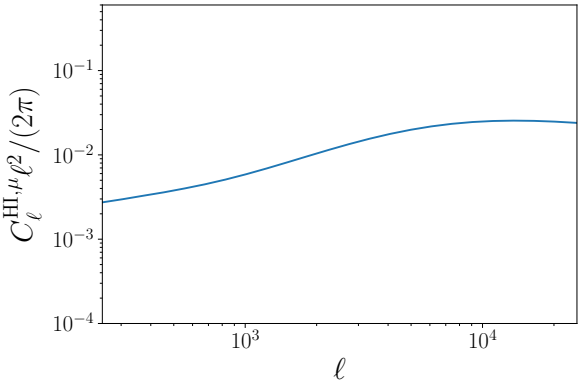

Figure 3. Our forecast for the HI-magnification cross correlation power spectrum. Same setup as in zhangpen but other α.

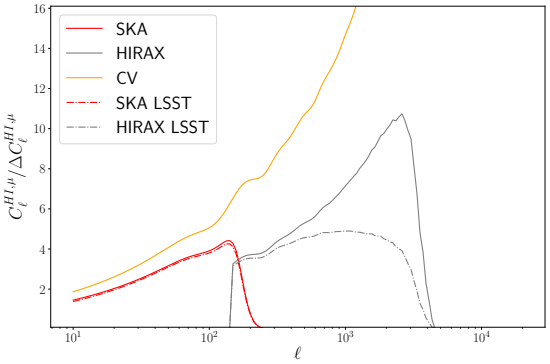

Figure 4. The signal to noise ratio for HIRAX and SKA both in the case of a perfect galaxy survey and assuming the galaxy number count of LSST. In the latter case we have not yet looked at the overlap of the surveys and simply assumed LSST to be all sky. The orange line is for an entirely cosmic variance limited experiment for both HI and galaxies. The grey lines are forecasts for HIRAX using the true baseline distribution, whereas the black line is using the simple fitting formula often used. Foreground redshift from 0.85 to 1.35 (same for HIRAX and SKA here for comparison) and background from 1.45 to 3.7. It is worth noting that the results for HIRAX are more strongly affected by the galaxy shot noise. I (Amadeus) think this is due to the shot noise being scale independent and thus dominating more on smaller scales, i.e. at the scales where HIRAX is operating (the power spectrum drops $\sim \ell^2$ for $\ell > 10^4$)

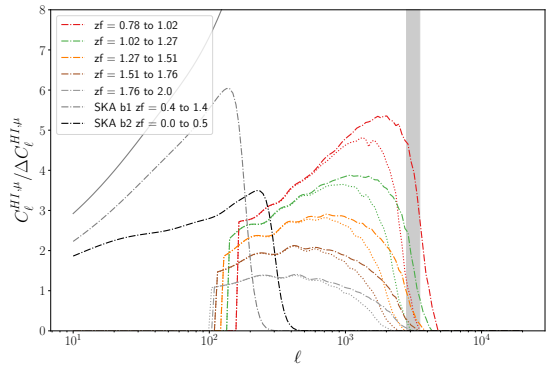

Figure 5. This should roughly be the main results plot. The solid grey line shows the highest cosmic variance limit of all foreground and background redshift combinations, and the grey shaded area indicates the start of nonlinear regime, which depends on redshift.

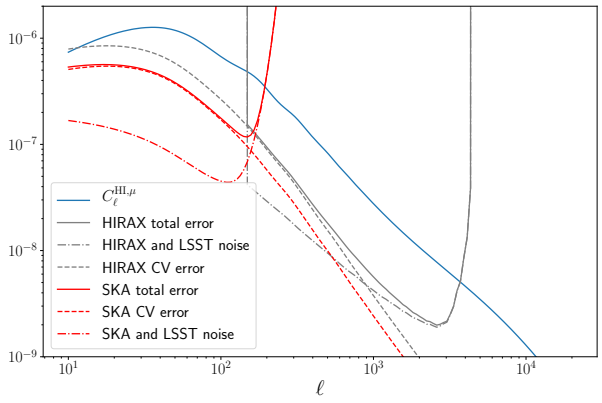

Figure 6. The different sources of error to $C_\ell^{\mathrm{HI},\mu}$ for both SKA and HIRAX.

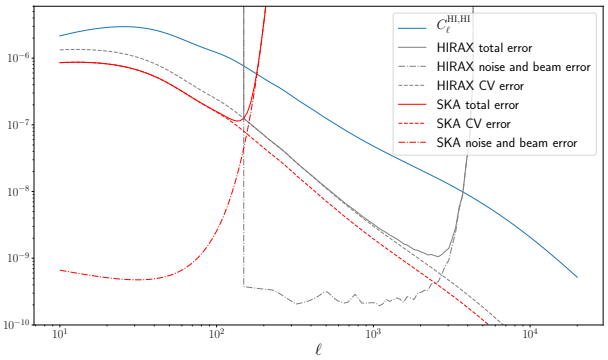

Figure 7. The different sources of error to $C_\ell^{\mathrm{HI-HI}}$ for both SKA and HIRAX.

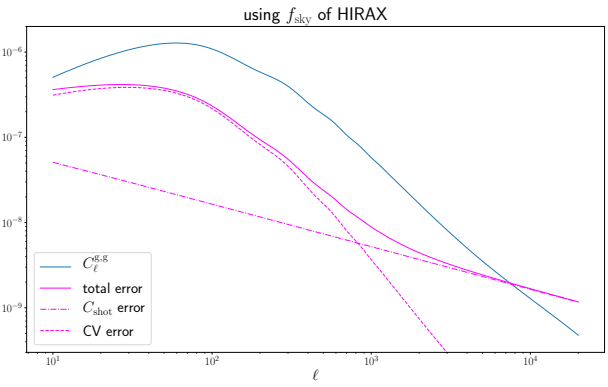

Figure 8. The different sources of error to C_ℓ^{gg} for both SKA and HIRAX.

5 DISCUSSION AND CONCLUSIONS

SKA and HIRAX combine well for magnification bias detection...

REFERENCES

Alonso D., Bull P., Ferreira P. G., Maartens R., Santos M. G., 2015, The Astrophysical Journal, 814, 145
Hall A., Bonvin C., Challinor A., 2013, Phys. Rev. D, 87, 064026
Limber D. N., 1954, ApJ, 119, 655
Loverde M., Afshordi N., 2008, Phys. Rev. D, 78, 123506
Scranton R., et al., 2005, ApJ, 633, 589
Ziour R., Hui L., 2008, Phys. Rev. D, 78, 123517